NEURAL REGENERATION RESEARCH
May 2015, Volume 10, Issue 5
www.nrronline.org

RESEARCH ARTICLE

Effective components of Chinese herbs reduce central nervous system function decline induced by iron overload

Xian-hui Dong[1], Jiang-tao Bai[1], Wei-na Kong[2], Xiao-ping He[3], Peng Yan[1], Tie-mei Shao[2], Wen-guo Yu[2], Xi-qing Chai[2,*], Yan-hua Wu[1], Cong Liu[1]

1 Chengde Medical University, Chengde, Hebei Province, China
2 Hebei Chemical and Pharmaceutical Vocational and Technical College, Shijiazhuang, Hebei Province, China
3 The 266 Hospital of Chinese PLA, Chengde, Hebei Province, China

***Correspondence to:**
Xi-qing Chai, M.D., xqchai@163.com.

***doi:**10.4103/1673-5374.156981*
***http:**//www.nrronline.org/*

***Accepted:** 2015-04-18*

Abstract

Abnormally increased levels of iron in the brain trigger cascade amplification in Alzheimer's disease patients, resulting in neuronal death. This study investigated whether components extracted from the Chinese herbs epimedium herb, milkvetch root and kudzuvine root could relieve the abnormal expression of iron metabolism-related protein in Alzheimer's disease patients. An $APP_{swe}/PS1_{\Delta E9}$ double transgenic mouse model of Alzheimer's disease was used. The intragastric administration of compounds from epimedium herb, milkvetch root and kudzuvine root improved pathological alterations such as neuronal edema, increased the number of neurons, downregulated divalent metal transporter 1 expression, upregulated ferroportin 1 expression, and inhibited iron overload in the cerebral cortex of mice with Alzheimer's disease. These compounds reduced iron overload-induced impairment of the central nervous system, indicating a new strategy for developing novel drugs for the treatment of Alzheimer's disease.

***Key Words:** nerve regeneration; neurodegenerative diseases; Alzheimer's disease; transgenic animal models; mice; epimedium herb; milkvetch root; kudzuvine root; divalent metal transporter 1; ferroportin 1; neural regeneration*

***Funding:** This research was supported by the National Natural Science Foundation of China, No. 81273983; the Natural Science Foundation of Hebei Province in China, No. C2010001471; the Scientific and Technological Research Youth Foundation of Colleges and Universities in Hebei Province of China, No. Q2012036; the Hebei Provincial Food and Drug Administration in China, No. PT2014053.*

Dong XH, Bai JT, Kong WN, He XP, Yan P, Shao TM, Yu WG, Chai XQ, Wu YH, Liu C (2015) Effective components of Chinese herbs reduce central nervous system function decline induced by iron overload. Neural Regen Res 10(5):778-785.

Introduction

Alzheimer's disease (AD) is a neurodegenerative disease related to age and characterized by progressive memory and cognitive dysfunction (Moloney et al., 2010; Zhang et al., 2014), but its pathogenesis remains unclear. Many theories have been suggested for the pathogenesis of AD, including gene mutation (Bettens et al., 2013), Aβ toxicity (Galante et al., 2012; Han et al., 2013), Tau protein aberrant modification, oxidative stress (Mohsenzadegan and Mirshafiey, 2012), inflammation (Azizi and Mirshafiey, 2012), cholinergic damage, lipid metabolism disorder (Lesser et al., 2009; Fernandez-Vizarra et al., 2012), neuronal apoptosis (Reddy and Beal), synaptic damage (Lister and Barnes, 2009), axonal transport disorders and endocrine disorders (Zhang et al., 2012), and metal ion metabolism disorder (Kong et al., 2013). As opinions on immune abnormalities (Bartos et al., 2012), viral infections (Nussbaum et al., 2013) and emotional factors (Ramakers et al., 2013) vary widely, no unanimous conclusion can be drawn (Hanger et al., 2009; Suo and Li, 2010). A study showed that the application of iron chelator deferoxamine could reduce the progression of AD, but caused some side effects and oral problems (Onor et al., 2007; Kadir et al., 2008).

The occurrence of AD is associated with age and aging (Sun and He, 2014; Wang et at., 2014). AD is a symptom of deficiency in origin and excess in superficiality, including renal deficiency, essence damage, and insufficiency of vital energy and blood as the origin, as well as intermingled phlegm and blood stasis and endogenous turbidity toxin as the superficiality (Lei and Li, 2012). Epimedium herb is a principal drug that belongs to liver and kidney meridians (Liu et al., 2014) and can invigorate the kidney, replenish essence (Kang et al., 2012), produce essence, and nourish marrow (China Pharmacopoeia Committee, 2005). Milkvetch root is a ministerial drug that belongs to lung and spleen meridians (Guo et al., 2013a), which can benefit vital energy (Tong, 2011), invigorate the spleen, and promote blood circulation for removing blood stasis (Zhang, 2012). Kudzuvine root is an adjuvant that belongs to spleen and stomach meridians, which can reduce fever, purge the

evil fire, expel toxin, increase the lucid yang and help drugs traffic to the head (Shi and Zhang, 2003). The combined use of the above three medicines can nourish the liver and kidney, invigorate the spleen, nourish blood, activate blood circulation to dissipate blood stasis, clear away the heat-evil and expel superficial evils, invigorate the brain and promote mentality. Therefore, the effective components of these herbs (icariin, astragalosides and puerarin) were combined into a prescription.

Cellular iron metabolism includes iron uptake and release. Divalent metal transporter 1 (DMT1) participates in cell Fe^{2+} uptake. DMT1 belongs to the natural resistance-associated macrophage protein family and has 12 membrane-spanning domains. The 3′-untranslational region of DMT1 mRNA with or without iron-response elements (IRE), DMT1 is divided into two isomers DMT1-with IRE and DMT1-without IRE. These isomers are located in the cell membrane and endocytic vesicle membrane of the intracellular loop and are involved in the uptake and transport of many divalent metal ions, particularly iron ions, and are important metal transporter proteins for maintaining intracellular divalent metal ion homeostasis (Shawki and Mackenzie, 2010). Ferroportin 1 (FPN1) mediates the transport of intracellular iron outside cells.

This study investigated the effects of a compound combining the effective components of epimedium herb, milkvetch root and kudzuvine root on DMT1 and FPN1 expression in the cerebral cortex of $APP_{swe}/PS1_{\Delta E9}$ double transgenic mouse model of AD using Nissl staining, immunohistochemistry and molecular biology methods.

The $APP_{swe}/PS1_{\Delta E9}$ mice express a mouse human hybrid transgene containing Swedish mutations (K594N/M595L) and deleted exon-9.

Materials and methods

Experimental groups and drug administration

A total of 60 specific-pathogen-free male $APP_{swe}/PS1_{\Delta E9}$ double transgenic mice aged 6 months were equally and randomly assigned to model, epimedium herb, milkvetch root, kudzuvine root, compound and deferoxamine groups. An additional 10 C57BL/6J mice (6 months old) served as negative controls (control group). All animals were purchased from Beijing HFK Bioscience Co., Ltd., China (license No. SCXK (Jing) 2014-0004). All mice were fed for 2 weeks for pre-feeding in individual cages in a 12-hour dark/light cycle at constant temperature, and allowed free access to food and water. This study was approved by the Ethics Committee of Hebei Medical University in China.

This study used three times the clinical dose of medication. Mice in the epimedium herb, milkvetch root, kudzuvine root and compound groups were given 120 mg/kg epimedium herb (Nanjing Zelang Pharmaceutical Co., Ltd., Nanjing, China), 80 mg/kg milkvetch root (Nanjing Zelang Pharmaceutical Co., Ltd.), 80 mg/kg kudzuvine root (Nanjing Zelang Pharmaceutical Co., Ltd.), 120 mg/kg epimedium herb + 80 mg/kg milkvetch root + 80 mg/kg kudzuvine root *via* intragastric administration, once a day, for 3 consecutive months. Mice in the deferoxamine group were intraperitoneally injected with 30 mg/kg deferoxamine, once a day, for 3 consecutive months (Guo et al., 2013a, b). Mice in the model and control groups were intragastrically administered 1 mL of PBS.

Sample collection

At 3 months after consecutive medication, three mice were collected from each group, and intraperitoneally anesthetized with 10% chloral hydrate. The chest was rapidly opened. Right atrial appendage and the apex of the heart were removed. Mice were perfused with physiological saline containing 1% heparin through the left ventricle into the ascending aorta until clear fluid was effused from the right atrial appendage until the extremities of the mouse limbs, lung and liver became white. Mice were then rapidly perfused with 0.1 M, 4°C, 4% paraformaldehyde. After perfusion for approximately 20 seconds, the speed of perfusion was slowed down. The perfusion lasted for 20 minutes. Mice were postfixed at 4°C for 2 hours. Brain tissue was obtained, fixed with 4% paraformaldehyde for 24 hours, and immersed in 30% sucrose solution. Tissue was serially sliced into 20-μm-thick sections at −25°C with a freezing microtome, and stored at −20°C for Nissl staining and immunohistochemistry. The remaining seven mice in each group were not perfused. The cerebral cortex was removed and cut into two parts along the median line. The left cerebral cortex was used for real time-PCR and the right cerebral cortex was used for western blot assay.

Morphology of mouse cortical neurons observed by Nissl staining

Ten frozen sections were selected from each group, heated at 46°C for 2 hours, washed three times with distilled water, each for 5 minutes, stained with 2% thionine preheated to 60°C for 30 minutes, rapidly washed with distilled water, treated with 95% ethanol, dehydrated with anhydrous ethanol, permeabilized with xylene, mounted with neutral resin, and observed by light microscopy (Wetzlar GmbH, AltenbergerStr. Solms, Germany). Ten fields were selected under a high power lens. The number of nerve cells was counted in each group.

DMT1 and FPN1 expression in mouse cerebral cortex as detected by immunohistochemistry

Ten frozen sections were selected from each group, heated at 46°C for 2 hours, washed three times with PBS, each for 5 minutes, treated with 3% H_2O_2, blocked with goat serum, incubated with rabbit anti-mouse DMT1-with/without IRE (1:3,000; Alpha Diagnostics, Owings Mills, MD, USA) and FPN1 primary antibody (1:3,000; Alpha Diagnostics, San Antonio, TX, USA). PBS, instead of primary antibody, was used as a negative control, at 4°C overnight. Sections were subsequently incubated with goat anti-rabbit biotinylated secondary antibody (Biotin-Streptavidin HRP Detection Systems, ZSGB-BIO, Beijing, China) at 37°C for 15 minutes, incubated with HRP-labeled streptavidin at 37°C for 15 minutes, visualized with 3,3′-diaminobenzidine, counterstained, dehydrated, permeabilized, mounted, and observed by light

Table 1 Primer sequences used in real-time PCR

Gene	Primer sequence	Annealing temperature (°C)	Product size (bp)
β-Actin	Forward: 5′-ACA GCT TCT TTG CAG CTC CTT C-3′ Reverse: 5′-CCA CGA TGG AGG GGA ATA CAG-3′	57	159
DMT1	Forward: 5′-GTG CGG GAA GCC AAT AAG TA-3′ Reverse: 5′-TCA CTG GGA AAG AGG TCA GC-3′	57	179
FPN1	Forward: 5′-TGG ATG GGT CCT TAC TGT CTG-3′ Reverse: 5′-TCT CCT GCC ACA ACA ACA ATC-3′	55	120

DMT1: Divalent metal transporter; FPN1: ferroportin 1.

microscopy. Five fields of each section (magnification, × 400) were selected and the mean number of positive cells in each field was calculated.

DMT1 and *FPN1* mRNA expression in mouse cerebral cortex as measured by real-time PCR

The left cerebral cortex was obtained from each mouse. Total RNA was extracted by the Trizol method. Optical density was measured at 260 and 280 nm using an ultraviolet spectrophotometer (Beckman Coulter, Kraemer Boulevard Brea, CA, USA). The purity and concentration of total RNA were calculated. Using the M-MLV First-Strand Synthesis System (Invitrogen, Prom-Test LLC, Koghbatsi 28/69, 0014, Yerevan, Armenia), 1 μg of total RNA was added to a mixture of oligo$(dT)_{20}$ 1 μL and 10 mM dNTP 1 μL, 5 × buffer 2 μL, and RNase-free water, up to 10 μL. Samples were degenerated at 65°C for 5 minutes, cooled on ice, centrifuged briefly, then PrimeScript RT Enzyme 2 μL and 0.1 M DTT 1 μL were added, blended at 37°C for 2 minutes, incubated with M-MLV reverse transcriptase, and stirred at 37°C for 5 minutes. The reaction product was stored at −20°C. Primers were designed and synthesized by Invitrogen in accordance with the sequences of *DMT1* and *FPN1* genes in GenBank (DMT1: http://www.ncbi.nlm.nih.gov/gene/18174; FPN1: http://www.ncbi.nlm.nih.gov/gene/53945). The primer sequences are shown in **Table 1**.

Using the Platinum SYBR Green qPCRSuperMix-UDG with ROX (Invitrogen) real-time PCR Kit, cDNA samples in five concentration gradients at five-fold dilution were obtained. Standard curves of the target gene and β-actin gene amplification were established and their amplification efficiency was identified. A 25-μL volume reaction system consisted of SYBR Ex Taq 12.5 μL, upstream primer (10 μM) 0.5 μL, downstream primer (10 μM) 0.5 μL, cDNA (10 μM) 0.5 μL and ddH_2O 11 μL. Amplification conditions were predenaturation at 95°C for 3 minutes, denaturation at 95°C for 30 seconds, annealing for 30 seconds, and elongation at 72°C for 30 seconds for 40 cycles. Fluorescence was measured after each cycle. To identify the specificity of amplificaiton, melting curves were analyzed after cycling. Conditions were as follows: 65–95°C, increasing 0.5°C every 5 seconds. In each group of samples, template wells without cDNA were used as negative controls. Experiments in each sample were performed in triplicate. The relative copy number of each sample was determined using BioRad Manager™ software (Bio-Rad Laboratories, Philadelphia, Armenia). Relative expression levels were calculated using the $2^{-\Delta\Delta Ct}$ method.

DMT1-with IRE, DMT1-without IRE and FPN1 protein expression in mouse cerebral cortex as detected by western blot assay

The right cerebral cortex was obtained to extract total protein. Protein was quantified using the bicinchoninic acid method. A total of 50 μg protein was loaded on the gel for 2 hours of electrophoresis and then transferred to 0.45 μm polyvinylidene difluoride membranes at a constant current for 2 hours. The membrane was blocked with 5% milk for 2 hours, incubated with primary rabbit anti-β-actin antibody (1:5,000; HangZhou HuaAn Biotechnology Co., Ltd., Hangzhou, China), rabbit anti-rat DMT1-with IRE (1:3,000; Alpha Diagnostics, Owings Mills, MD, USA), rabbit anti-rat DMT1-without IRE (1:2,000; Alpha Diagnostics) and rabbit anti-mouse FPN1 (1:3,000; Alpha Diagnostics) at 4°C overnight, washed three times with Tris-buffered saline and Tween, each for 5 minutes, incubated with secondary antibody goat anti-rabbit (1:10,000; KPL, Gaithersburg, MD, USA) at room temperature for 1 hour, and washed three times with 0.05% Tris-buffered saline and Tween. DMT1-with IRE, DMT1-without IRE and FPN1 protein expressions were detected using a photochemical chromogenic method. β-Actin was used as an internal reference. The optical density of protein bands was analyzed using Quantity One analysis software (Bio-Rad Laboratories). The protein expression was expressed as the optical density ratio of target protein to β-actin.

Statistical analysis

All data are expressed as the mean ± SD and were statistically processed using SPSS 17.0 software (SPSS, Chicago, IL, USA). Intergroup differences were compared by multivariate analysis of variance followed by the least significant difference test. A value of $P < 0.05$ was considered statistically significant.

Results

A compound of the effective components of epimedium herb, milkvetch root and kudzuvine root improved neuronal morphology in the cerebral cortex of AD transgenic mice

Nissl staining demonstrated that in the control group, nerve cells were arranged neatly and densely, abundant Nissl bodies were visible in the cytoplasm, Nissl bodies were present as dark blue staining, and nuclei were light blue in the cerebral cortex of mice. In the model group, neuronal swelling was

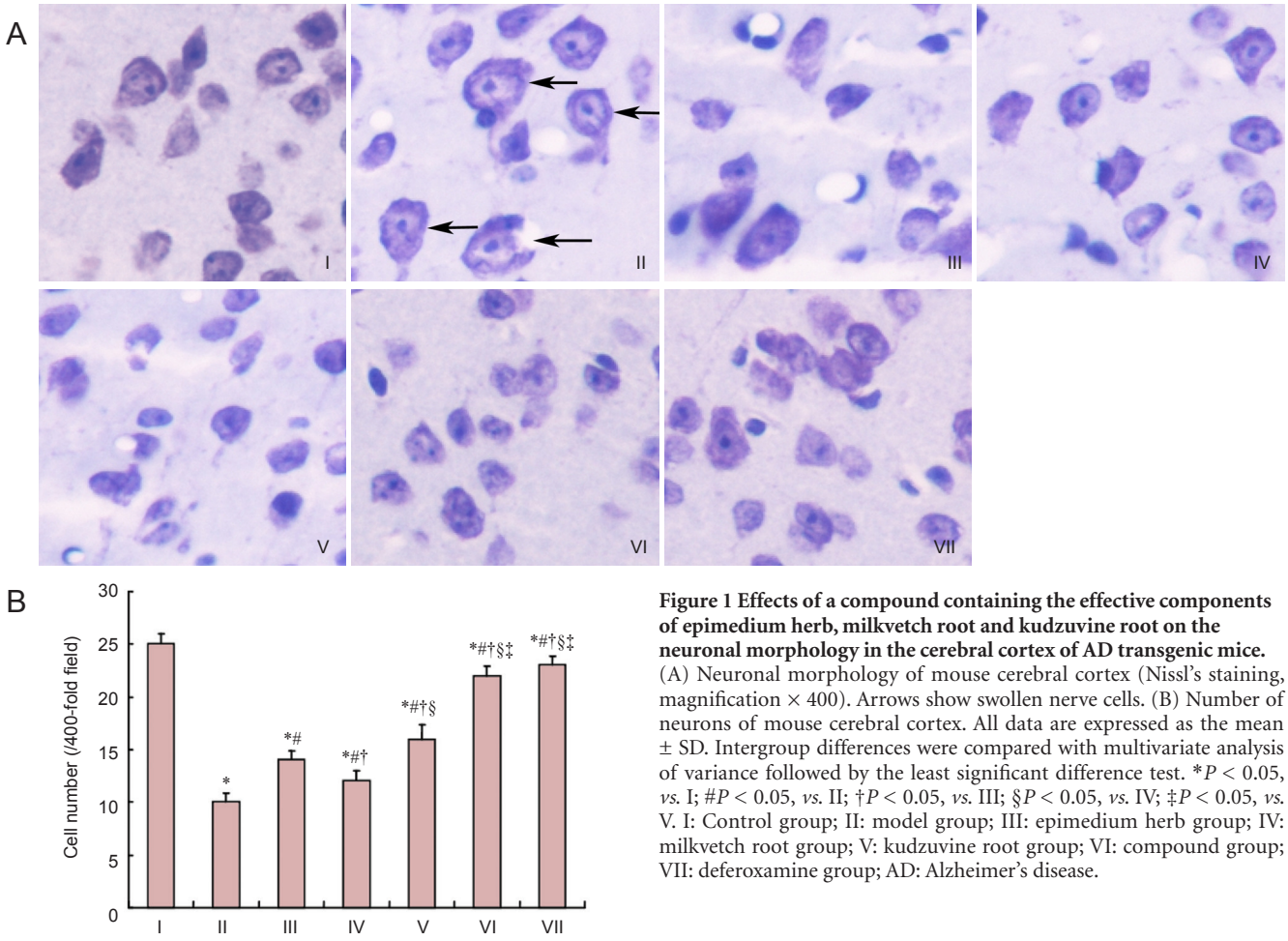

Figure 1 Effects of a compound containing the effective components of epimedium herb, milkvetch root and kudzuvine root on the neuronal morphology in the cerebral cortex of AD transgenic mice.
(A) Neuronal morphology of mouse cerebral cortex (Nissl's staining, magnification × 400). Arrows show swollen nerve cells. (B) Number of neurons of mouse cerebral cortex. All data are expressed as the mean ± SD. Intergroup differences were compared with multivariate analysis of variance followed by the least significant difference test. *$P < 0.05$, *vs.* I; #$P < 0.05$, *vs.* II; †$P < 0.05$, *vs.* III; §$P < 0.05$, *vs.* IV; ‡$P < 0.05$, *vs.* V. I: Control group; II: model group; III: epimedium herb group; IV: milkvetch root group; V: kudzuvine root group; VI: compound group; VII: deferoxamine group; AD: Alzheimer's disease.

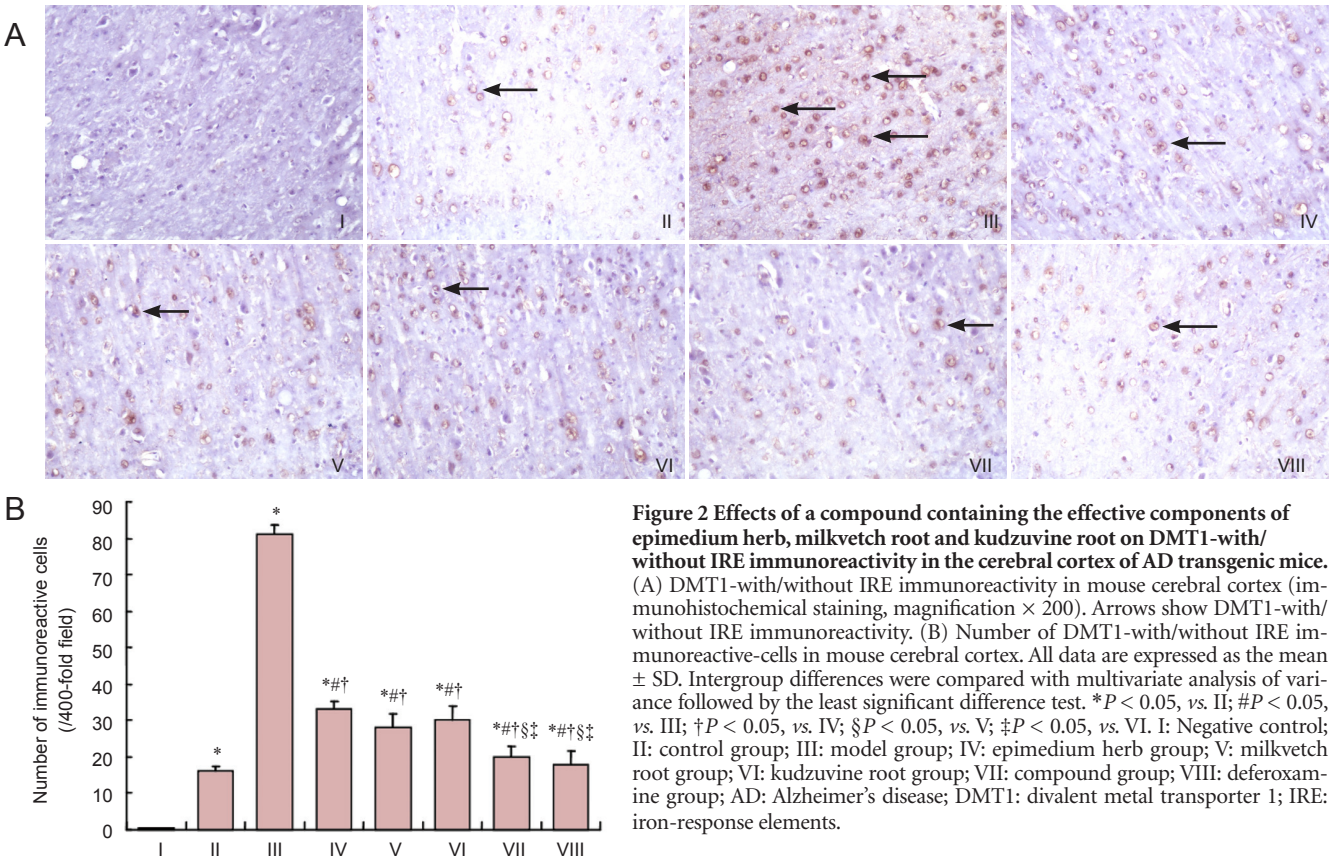

Figure 2 Effects of a compound containing the effective components of epimedium herb, milkvetch root and kudzuvine root on DMT1-with/without IRE immunoreactivity in the cerebral cortex of AD transgenic mice.
(A) DMT1-with/without IRE immunoreactivity in mouse cerebral cortex (immunohistochemical staining, magnification × 200). Arrows show DMT1-with/without IRE immunoreactivity. (B) Number of DMT1-with/without IRE immunoreactive-cells in mouse cerebral cortex. All data are expressed as the mean ± SD. Intergroup differences were compared with multivariate analysis of variance followed by the least significant difference test. *$P < 0.05$, *vs.* II; #$P < 0.05$, *vs.* III; †$P < 0.05$, *vs.* IV; §$P < 0.05$, *vs.* V; ‡$P < 0.05$, *vs.* VI. I: Negative control; II: control group; III: model group; IV: epimedium herb group; V: milkvetch root group; VI: kudzuvine root group; VII: compound group; VIII: deferoxamine group; AD: Alzheimer's disease; DMT1: divalent metal transporter 1; IRE: iron-response elements.

observed and the number of cells were decreased. Cells were arranged sparsely and the intercellular space was increased. Intracytoplasmic Nissl bodies were reduced with unclear boundaries, and were stained light blue. Neuronal swelling was relieved, and the number of cells slightly increased in the epimedium herb, milkvetch root and kudzuvine root groups compared with the model group. In the compound and deferoxamine groups, nerve cells were arranged regularly and densely in the cerebral cortex, with the presence of abundant Nissl bodies in the cytoplasm, improving swelling and increasing the number of cells (**Figure 1**).

Effects of a compound of the effective components of epimedium herb, milkvetch root and kudzuvine root on DMT1 and FPN1 expression in the cerebral cortex of AD transgenic mice

Immunohistochemical staining results revealed that DMT1-with/without IRE expression was higher ($P < 0.05$), and FPN1 expression was lower ($P < 0.05$) in the cerebral cortex of the model group compared with the control group. DMT1-with/without IRE expression was lower in the epimedium herb, milkvetch root, kudzuvine root, compound and deferoxamine groups than in the model group ($P < 0.05$). FPN1 expression was higher in the epimedium herb, milkvetch root, kudzuvine root, compound and deferoxamine groups than in the model group ($P < 0.05$). DMT1-with/without IRE expression was higher ($P < 0.05$), but FPN1 expression was lower ($P < 0.05$) in the epimedium herb, milkvetch root and kudzuvine root groups compared with the deferoxamine group. No significant difference was detected in DMT1-with/without IRE and FPN1 expression in mouse cerebral cortex between deferoxamine and compound groups ($P > 0.05$; **Figures 2**, **3**).

Effects of the compound of the effective components of epimedium herb, milkvetch root and kudzuvine root on *DMT1* and *FPN1* mRNA expression in the cerebral cortex of AD transgenic mice

Real time-PCR results indicated that *DMT1* mRNA expression was higher ($P < 0.05$), and that *FPN1* mRNA expression was lower ($P < 0.05$) in the cerebral cortex of the model group compared with the control group. *DMT1* mRNA expression was lower ($P < 0.05$) and *FPN1* mRNA expression was higher ($P < 0.05$) in the epimedium herb, milkvetch root, kudzuvine root, compound and deferoxamine groups compared with the model group. *DMT1* mRNA expression was higher ($P < 0.05$), and *FPN1* mRNA expression was lower ($P < 0.05$) in the epimedium herb, milkvetch root, and kudzuvine root groups compared with the deferoxamine group. No significant difference in *DMT1* mRNA and *FPN1* mRNA expression was detected between compound and deferoxamine groups ($P > 0.05$; **Figure 4**).

Effects of the compound of effective components of epimedium herb, milkvetch root and kudzuvine root on DMT1-with IRE, DMT1-without IRE and FPN1 expression in the cerebral cortex of AD transgenic mice

Western blot assay indicated that DMT1-with IRE and DMT1-without IRE expression was higher ($P < 0.05$) and that FPN1 expression was lower ($P < 0.05$) in the model group compared with the control group. DMT1-with IRE and DMT1-without IRE expression was lower ($P < 0.05$) and FPN1 expression was higher ($P < 0.05$) in the epimedium herb, milkvetch root, kudzuvine root, compound and deferoxamine groups compared with the model group. DMT1-with IRE and DMT1-without IRE expression was higher ($P < 0.05$) and FPN1 expression was lower ($P < 0.05$) in the epimedium herb, milkvetch root and kudzuvine root groups compared with the deferoxamine group. No significant difference in DMT1-with IRE and DMT1-without IRE and FPN1 expression was observed between the compound and deferoxamine groups ($P > 0.05$; **Figure 5**). Western blot assay results were consistent with the results of real-time PCR.

Discussion

Iron levels increase abnormally in AD patients (Sun et al., 2010). The increase in iron content might be associated with the abnormal expression of iron metabolism-related proteins in the brain tissues of AD patients (Colangelo et al., 2002; Zhang et al., 2008). DMT1 and FPN1 are important iron metabolism-related proteins in brain tissues.

Gruenheid et al. (1995) found nature resistance-associated macrophage protein 2 (Nramp2), has a high homology and similar secondary structure to Nramp1. Because Nramp2 can transport divalent cations, it is also called divalent metal ion transporter. DMT1 belongs to the Nramp family. The abnormal expression of DMT1 might be a cause of neurodegenerative diseases. The relationship of DMT1 and AD remains unclear. Previous studies demonstrated that DMT1 expression had an increasing trend with age in the brain of aged rats and various inflammatory factors also upregulated DMT1 expression in the brain (Lee et al., 1998; Mackenzie et al., 2007). These two conditions are important risk factors for AD. Nevertheless, there have been no reports of a correlation of DMT1 and pathogenesis of AD. FPN1 is a transmembrane iron export protein mainly located in the basal and basolateral membranes of duodenal epithelial cells. FPN1 is the only outlet for iron ion release and is responsible for intracellular iron transport out of cells (Urrutia et al., 2013; Yu et al., 2013).

Abnormally increased iron in the brain triggers a cascade amplification mechanism, resulting in neuronal death. Iron plays an important role in the occurrence and development of AD. Iron chelators such as deferoxamine reduced the progression of AD, but these chemicals have toxicity and are difficult to administer orally. Therefore, in accordance with the principle of treating both manifestation and root cause of disease, this study investigated the active components of epimedium herb, milkvetch root and kudzuvine root, including icariin (Zhang et al., 2014a, b), astragalosides (Sun et al., 2014) and puerarin (Wang et al., 2014a). A clinical study confirmed that after taking epimedium herb, milkvetch root and kudzuvine root for 3 months, the intelligence and memory of AD patients and daily living skills were enhanced with no significant adverse events or side effects (Li et al., 2005).

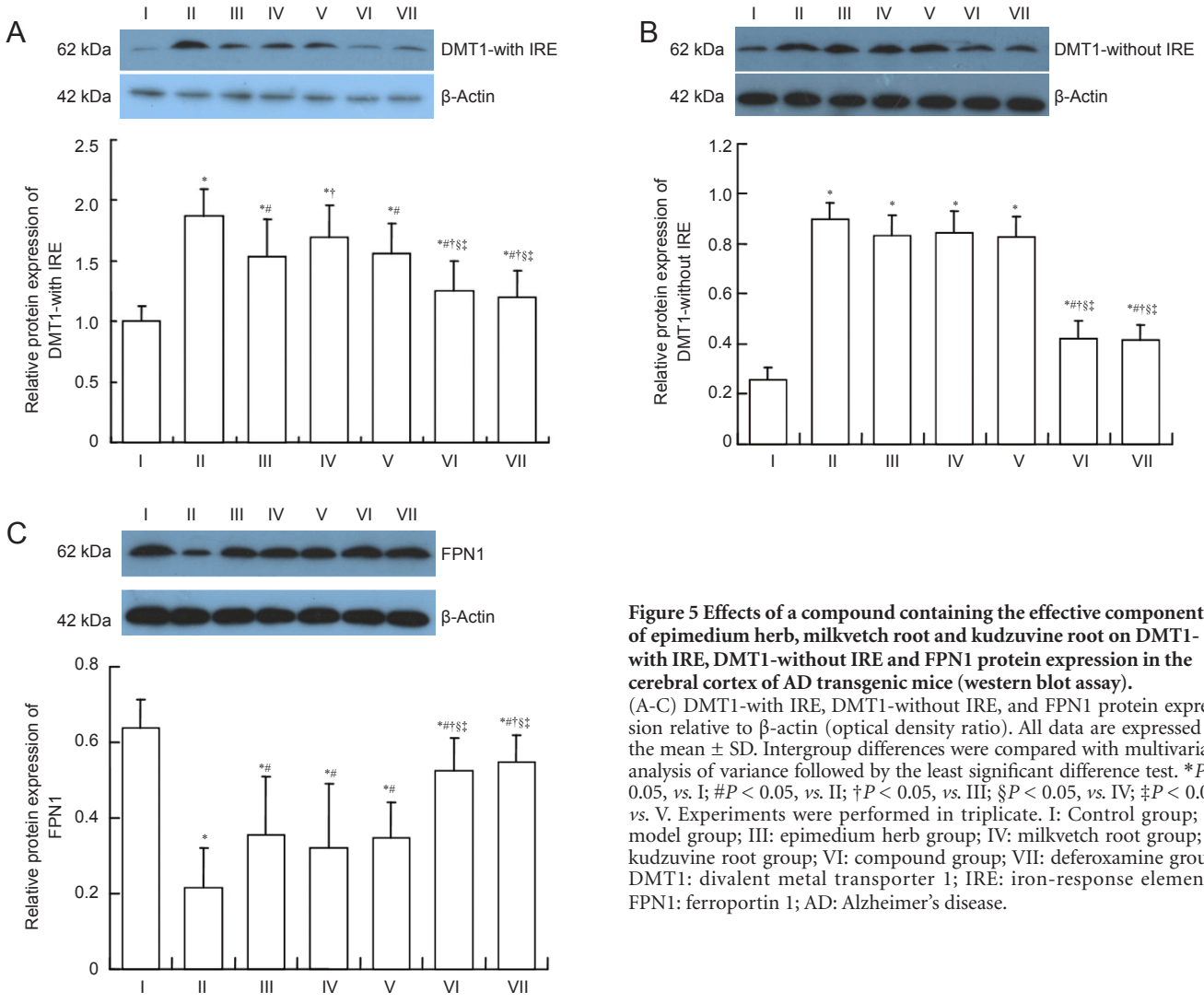

Figure 5 Effects of a compound containing the effective components of epimedium herb, milkvetch root and kudzuvine root on DMT1-with IRE, DMT1-without IRE and FPN1 protein expression in the cerebral cortex of AD transgenic mice (western blot assay).
(A-C) DMT1-with IRE, DMT1-without IRE, and FPN1 protein expression relative to β-actin (optical density ratio). All data are expressed as the mean ± SD. Intergroup differences were compared with multivariate analysis of variance followed by the least significant difference test. *$P <$ 0.05, *vs.* I; #$P < 0.05$, *vs.* II; †$P < 0.05$, *vs.* III; §$P < 0.05$, *vs.* IV; ‡$P < 0.05$, *vs.* V. Experiments were performed in triplicate. I: Control group; II: model group; III: epimedium herb group; IV: milkvetch root group; V: kudzuvine root group; VI: compound group; VII: deferoxamine group; DMT1: divalent metal transporter 1; IRE: iron-response elements; FPN1: ferroportin 1; AD: Alzheimer's disease.

Numerous studies using modern pharmacological methods have investigated the mechanisms of icariin (Nie et al., 2008), astragalosides (Zhang et al., 2007) and puerarin (Wang et al., 2009) for the treatment of AD. However, these studies mainly explored the effects of icariin, astragalosides and puerarin on neurotransmitters, oxidative stress, inflammatory reactions and Aβ metabolism in the brain, but did not study the effect on improving iron overload in the brain. The abnormal accumulation of iron in the brain of AD patients, as a endotoxin, plays an important role in the occurrence and development of AD, but the reason for the increase in iorn levels in the brain of AD patients remains unclear. We hypothesized that kidney deficiency and damage of essence might cause an abnormal accumulation of iron in the brain, suppress the primordial spirit, and thus the body could not abolish the poison. Moreover, the heart, liver and spleen might be weak and *Qi*-blood circulation abnormal; therefore, iron toxicity might not be effectively removed but be retained in the brain. Abundant iron accumulation induces damage to spiritual mechanisms (Guo et al., 2013b). These findings are consistent with the abnormal expression of some iron metabolism-related proteins in the brain of AD patients (Xian-hui et al., 2014). Taken together, a compound containing epimedium herb, milkvetch root and kudzuvine root might invigorate the kidney and spleen, produce essence, nourish marrow, benefit vital energy, nourish blood, wash away phlegm, remove blood stasis, adjust *Qi*, support healthy energy to eliminate evils, and finally remove iron toxicity. Pharmacological studies have demonstrated that the epimedium herb enhances the secretory function of the hypothalamic-pituitary-gonadal axis, adrenal axis, and thymus axis (He and Gu, 2014). Milkvetch root increases blood flow, improves cerebral ischemia and hypoxia, and resists oxidation (He and Gu, 2014). Kudzuvine root reduces blood glucose and blood lipid, decreases blood viscosity, improves microcirculation, and diminishes the risk of atherosclerosis (Li et al., 2006). These data lay a theoretical foundation for Chinese and Western medicine for the treatment of AD.

In summary, an $APP_{swe}/PS1_{\Delta E9}$ double transgenic mouse model of AD was used (Kemppainen et al., 2014; Wang et al., 2014b) and immunohistochemistry and molecular biology methods were utilized to investigate the effects of a compound containing the effective components of epimedium herb, milkvetch root and kudzuvine root on alterations in neurons,

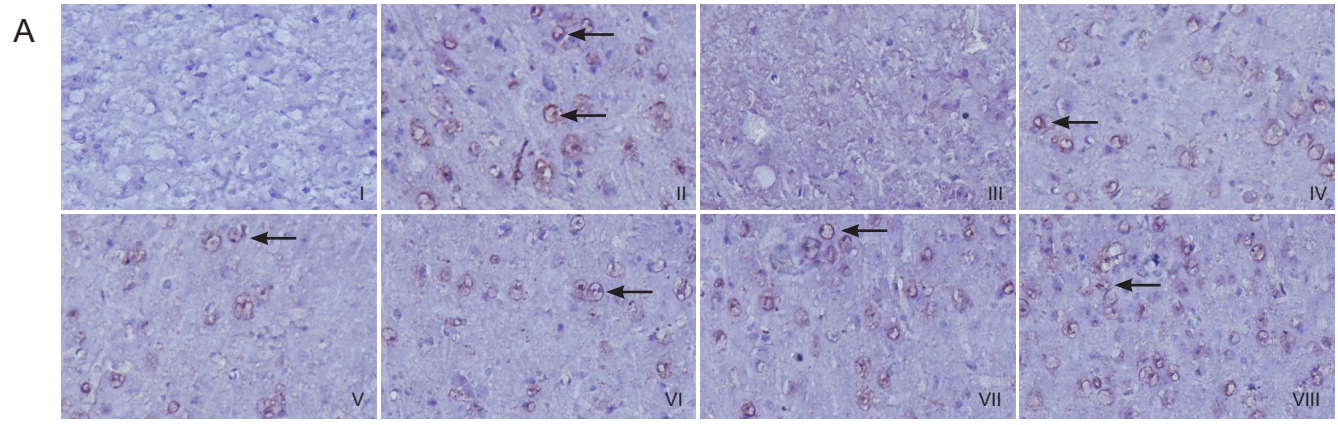

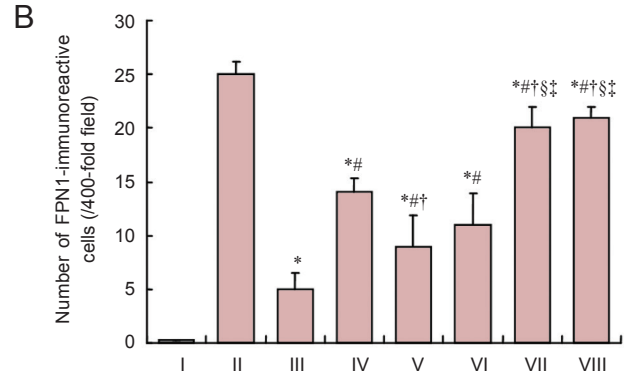

Figure 3 Effects of a compound containing the effective components of epimedium herb, milkvetch root and kudzuvine root on FPN1 immunoreactivity in the cerebral cortex of AD transgenic mice.
(A) FPN1 expression in mouse cerebral cortex (immunohistochemical staining, magnification × 400). Arrows show FPN1-immunoreactive cells. (B) Number of FPN1-immunoreactive cells in mouse cerebral cortex. All data are expressed as the mean ± SD. Intergroup differences were compared with multivariate analysis of variance followed by the least significant difference test. *$P < 0.05$, *vs.* II; #$P < 0.05$, *vs.* III; †$P < 0.05$, *vs.* IV; §$P < 0.05$, *vs.* V; ‡$P < 0.05$, *vs.* VI. I: Negative control; II: control group; III: model group; IV: epimedium herb group; V: milkvetch root group; VI: kudzuvine root group; VII: compound group; VIII: deferoxamine group; FPN1: ferroportin 1; AD: Alzheimer's disease.

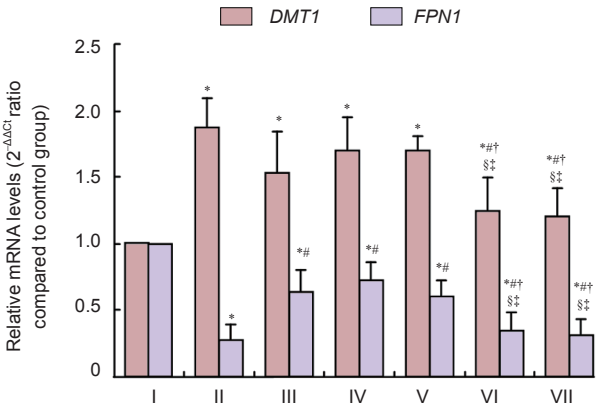

Figure 4 Effects of a compound containing the effective components of epimedium herb, milkvetch root and kudzuvine root on *DMT1* and *FPN1* mRNA expression in the cerebral cortex of AD transgenic mice (real-time PCR).
All data are expressed as the mean ± SD. Intergroup differences were compared with multivariate analysis of variance followed by the least significant difference test. *$P < 0.05$, *vs.* I; #$P < 0.05$, *vs.* II; †$P < 0.05$, *vs.* III; §$P < 0.05$, *vs.* IV; ‡$P < 0.05$, *vs.* V. Experiments were performed in triplicate. I: Control group; II: model group; III: epimedium herb group; IV: milkvetch root group; V: kudzuvine root group; VI: compound group; VII: deferoxamine group; *DMT1*: divalent metal transporter 1; *FPN1*: ferroportin 1; AD: Alzheimer's disease.

and DMT1 and FPN1 expression in the cerebral cortex of a mouse model of AD. Neuronal loss was evident in the cerebral cortex of AD mice and its mechanism might be correlated with iron overload in the brain. The compound of effective components of epimedium herb, milkvetch root and kudzuvine root improved neuronal swelling, increased the number of neurons, downregulated DMT1 expression, upregulated FPN1 expression, inhibited iron overload in the cerebral cortex of AD mice, relieved central nervous system function decline induced by iron overload. Thus, this study provides a new strategy for developing novel medicines for treating AD.

Author contributions: *XHD provided data, ensured the integrity of the data and wrote the paper. JTB and YHW analyzed the data. WNK participated in study concept and design. XPH provided technical support. TMS and CL provided the data. WGY served as a principle investigator. XQC obtained the funding and served as a principle investigator. All authors approved the final version of the paper.*
Conflicts of interest: *None declared.*

References

Azizi G, Mirshafiey A (2012) The potential role of proinflammatory and antiinflammatory cytokines in Alzheimer disease pathogenesis. Immunopharmacol Immunotoxicol 34:881-895.
China Pharmacopoeia Committee (2005) Pharmacopoeia of the People's Republic of China. Beijing: Chemical Industry Press.
Colangelo V, Schurr J, Ball MJ, Pelaez RP, Bazan NG, Lukiw WJ (2002) Gene expression profiling of 12633 genes in Alzheimer hippocampal CA1: transcription and neurotrophic factor down-regulation and up-regulation of apoptotic and pro-inflammatory signaling. J Neurosci Res 70:462-473.
Fernandez-Vizarra P, Lopez-Franco O, Mallavia B, Higuera-Matas A, Lopez-Parra V, Ortiz-Muñoz G, Ambrosio E, Egido J, Almeida OF, Gomez-Guerrero C (2012) Immunoglobulin G Fc receptor deficiency prevents Alzheimer-like pathology and cognitive impairment in mice. Brain 135:2826-2837.

Guo C, Wang T, Zheng W, Shan ZY, Teng WP, Wang ZY (2013a) Intranasal deferoxamine reverses iron-induced memory deficits and inhibits amyloidogenic APP processing in a transgenic mouse model of Alzheimer's disease. Neurobiol Aging 34:562-575.
Guo C, Wang P, Zhong ML, Wang T, Huang XS, Li JY, Wang ZY (2013b) Deferoxamine inhibits iron induced hippocampal tau phosphorylation in the Alzheimer transgenic mouse brain. Neurochem Int 62:165-172.
Han HY Zhang YC, Ji SQ, Liang QM, Zhu SQ, Xue Z (2013) Integrin beta 1 inhibits long-term potentiation induced by amyloid beta-protein. Zhongguo Zuzhi Gongcheng Yanjiu 17:1959-1964.
Hanger DP, Anderton BH, Noble W (2009) Tau phosphorylation: the therapeutic challenge for neurodegenerative disease. Trends Mol Med 15:112-119.
He XL, Gu N (2014) Reviews on the studies of antiatherosclerosis effect of Astragalus polysaccharide. Shizhen Guoyi Guoyao 25:1463-1465.
Kadir A, Andreasen N, Almkvist O, Wall A, Forsberg A, Engler H, Hagman G, Lärksäter M, Winblad B, Zetterberg H, Blennow K, Långström B, Nordberg A (2008) Effect of phenserine treatment on brain functional activity and amyloid in Alzheimer's disease. Ann Neurol 63:621-631.
Kang X, Liu RH, Wang XJ (2012) Advances on studies of anti-osteoporosis applications and mechanisms by Herba Epimedii and Fructus Ligustri Lucidi. Zhongguo Shiyan Fangji Xue Zazhi 18:331-334.
Kemppainen S, Hämäläinen E, Miettinen PO, Koistinaho J, Tanila H (2014) Behavioral and neuropathological consequences of transient global ischemia in APP/PS1 Alzheimer model mice. Behav Brain Res 275:15-26.
Kong WN, Lei YH, Chang YZ (2013) The regulation of iron metabolism in the mononuclear phagocyte system. Expert Rev Hematol 6:411-418.
Lee PL, Gelbart T, West C, Halloran C, Beutler E (1998) The human Nramp2 gene: characterization of the gene structure, alternative splicing, promoter region and polymorphisms. Blood Cells Mol Dis 24:199-215.
Lei HT, Li XM (2012) Review of Chinese medine on Alzherimer's disease. Liaoning Zhongyiyao Daxue Xuebao 14:215-217.
Lesser GT, Haroutunian V, Purohit DP, Schnaider Beeri M, Schmeidler J, Honkanen L, Neufeld R, Libow LS (2009) Serum lipids are related to Alzheimer's pathology in nursing home residents. Dement Geriatr Cogn Disord 27:42-49.
Li LX, Sun LP, Wei JW, Liu JG (2005) Modified Yiqi Yangyin mixture in treating Alzheimer disease by differentiation of symptoms. Zhongguo Linchuang Kangfu 9:93-94.
Li QX, Zhong RJ, Hou HJ, Yao SQ, Jiao HC, Gong HR, Shen DJ, Wu Q (2006) Effect of Puerarin on blood lipid and the aorta expression of endothelin in diabetic rats. Zhonghua Gaoxueya Zazhi 14:627-631.
Lister JP, Barnes CA (2009) Neurobiological changes in the hippocampus during normative aging. Arch Neurol 66:829-833.
Liu XY, Zii H, Zheng HX, Zhang ZQ, Li KQ (2014) Tissues distribution of Icariin and its metabolites in kidney of osteoporosis model rats. Zhongguo Shiyan Fangji Xue Zazhi 20:125-128.
Mackenzie B, Takanaga H, Hubert N, Rolfs A, Hediger MA (2007) Functional properties of multiple isoforms of human divalent metal-ion transporter 1 (DMT1). Biochem J 403:59-69.
Moloney AM, Griffin RJ, Timmons S, O'Connor R, Ravid R, O'Neill C (2010) Defects in IGF-1 receptor, insulin receptor and IRS-1/2 in Alzheimer's disease indicate possible resistance to IGF-1 and insulin signalling. Neurobiol Aging 31:224-243.
Nie J, Luo Y, Huang XN, Lu YF, Sun AS, Gong QH, Shi JS (2008) Protective effects of icariin on learning and memory dysfunction induced by amyloid β-protein fragment 25-35. Zhongguo Yaoli Xue yu Duli Xue Zazhi 22:31-37.
Nussbaum JM, Seward ME, Bloom GS (2013) Alzheimer disease: a tale of two prions. Prion 7:14-19.
Onor ML, Trevisiol M, Aguglia E (2007) Rivastigmine in the treatment of Alzheimer's disease: an update. Clin Interv Aging 2:17-32.
Reddy PH, Beal MF Amyloid beta, mitochondrial dysfunction and synaptic damage: implications for cognitive decline in aging and Alzheimer's disease. Trends Mol Med 14:45-53.
Shawki A, Mackenzie B (2010) Interaction of calcium with the human divalent metal-ion transporter-1. Biochem Biophys Res Commun 393:471-475.
Shi RL, Zhang JJ (2003) Protective effect of puerarin on vascular endothelial cell apoptosis induced by chemical hypoxia in vitro. Yao Xue Xue Bao 38:103-107.
Sun GJ, He YJ (2014) Progress in clinical research of traditional Chinese medicine on Alzheimer's disease. Zhongguo Zhongyiyao Xiandai Yuancheng Jiaoyu 12:164-165.
Sun Q, Jia N, Wang W, Jin H, Xu J, Hu H (2014) Protective effects of astragaloside IV against amyloid beta1-42 neurotoxicity by inhibiting the mitochondrial permeability transition pore opening. PLoS One 9:e98866.
Sun YM, Kong WN, Li GZ, Chai XQ (2010) High brain iron in etiology of Alzheimer's disease and therapeutic approaches. Zhongguo Yaoli Xue Tongbao 26:824-827.
Suo WZ, Li L (2010) Dysfunction of G protein-coupled receptor kinases in Alzheimer's disease. ScientificWorldJournal 10:1667-1678.
Tong X (2011) The pharmacology study of active constituents from Astragalus. Shizhen Guoyi Guoyao 22:1246-1249.
Urrutia P, Aguirre P, Esparza A, Tapia V, Mena NP, Arredondo M, González-Billault C, Núñez MT (2013) Inflammation alters the expression of DMT1, FPN1 and hepcidin, and it causes iron accumulation in central nervous system cells. J Neurochem 126:541-549.
Wang C, Xie N, Zhang H, Li Y, Wang Y (2014a) Puerarin protects against β-amyloid-induced microglia apoptosis via a PI3K-dependent signaling pathway. Neurochem Res 39:2189-2196.
Wang D, Liu L, Zhu X, Wu W, Wang Y (2014b) Hesperidin alleviates cognitive impairment, mitochondrial dysfunction and oxidative stress in a mouse model of Alzheimer's disease. Cell Mol Neurobiol 34:1209-1221.
Wang WS, Chai XQ, Wang YJ, Han M, Wen J (2009) Aβ-induced inflammatory response in hippocampus of rat and the suppressing effect of puerarin on it. Zhongguo Quanke Yixue 12:461-464.
Wang Z, Ren XQ, Wei DX (2014) Hippocampus transplantation of bone marrow mesenchymal stem cells improves the memory function of Alzheimer's disease rats. Zhongguo Zuzhi Gongcheng Yanjiu 18:8130-8134.
Xian-hui D, Wei-juan G, Tie-mei S, Hong-lin X, Jiang-tao B, Jing-yi Z, Xi-qing C (2015) Age-related changes of brain iron load changes in the frontal cortex in APPswe/PS1ΔE9 transgenic mouse model of Alzheimer's disease. J Trace Elem Med Biol 38:118-123.
Yu X, Du T, Song N, He Q, Shen Y, Jiang H, Xie J (2013) Decreased iron levels in the temporal cortex in postmortem human brains with Parkinson disease. Neurology 80:492-495.
Zhang GL (2012) Chinese medicine Huangqi pharmacological functions and clinical application research. Shiyong Xin Nao Fei Xueguan Bing Zazhi 20:1059-1060.
Zhang L, Shen C, Chu J, Zhang R, Li Y, Li L (2014a) Icariin decreases the expression of APP and BACE-1 and reduces the β-amyloid burden in an APP transgenic mouse model of Alzheimer's disease. Int J Biol Sci 10:181-191.
Zhang LH, Wang X, Stoltenberg M, Danscher G, Huang L, Wang ZY (2008) Abundant expression of zinc transporters in the amyloid plaques of Alzheimer's disease brain. Brain Res Bull 77:55-60.
Zhang N, Du HJ, Wang JH, Cheng Y (2012) A pilot study on the relationship between thyroid status and neuropsychiatric symptoms in patients with Alzheimer disease. Chin Med J (Engl) 125:3211-3216.
Zhang SP, Xuan ZB, Huang ZY, Liu YQ, Liu Q, Wang XY, Wu CJ, Yang LM, Abbas Z (2014) The association between angiotensin converting enzyme gene polymorphism and Alzheimer's disease in Jiamusi region. Zhongguo Zuzhi Gongcheng Yanjiu 18:259-264.
Zhang YL, Liu DM, Wu QS, Yao YY, Li WP (2007) Effect of the extract of astragalus on the ability of learning and memory and the expression of Bcl-2 and Bcl-xl protein of the hippocampal neurons in rat model of Alzheimer's disease. Anhui Yike Daxue Xuebao 42:299-302.
Zhang ZY, Li C, Zug C, Schluesener HJ (2014b) Icariin ameliorates neuropathological changes, TGF-β1 accumulation and behavioral deficits in a mouse model of cerebral amyloidosis. PLoS One 9:e104616.

Copyedited by Croxford L, Raye W, Yu J, Qiu Y, Li CH, Song LP, Zhao M